AIAA 2004-0821

Thermal Resistances of Gaseous Gap for Conforming Rough Contacts

M. Bahrami, J. R. Culham and M. M. Yovanovich
Microelectronics Heat Transfer Laboratory
Department of Mechanical Engineering, University of Waterloo
Waterloo, Ontario, Canada N2L 3G1

42nd AIAA Aerospaces Meeting and Exhibit
Jan 5-8, 2004/Reno, Nevada

Thermal Resistances of Gaseous Gap for Conforming Rough Contacts

M. Bahrami*, J. R. Culham†and M. M. Yovanovich‡
Microelectronics Heat Transfer Laboratory
Department of Mechanical Engineering, University of Waterloo
Waterloo, Ontario, Canada N2L 3G1

An approximate analytical model is developed for predicting the heat transfer of interstitial gases in the gap between conforming rough contacts. A simple relationship for the gap thermal resistance is derived by assuming that the contacting surfaces are of uniform temperature and that the gap heat transfer area and the apparent contact area are identical. The model covers the four regimes of gas heat conduction modes, i.e., continuum, temperature-jump or slip, transition, and free molecular. Effects of main input parameters on the gap and joint thermal resistances are investigated. The model is compared with the existing model of Yovanovich et al. and with more than 510 experimental data points collected by Hegazy and Song. Good agreement is shown over entire range of the comparison.

Nomenclature

A	=	area, m^2
a	=	radius of contact, m
b_L	=	specimens radius, m
c_1	=	Vickers microhardness coefficient, Pa
c_2	=	Vickers microhardness coefficient
d	=	mean contacting bodies distance, m
F	=	external force, N
h	=	contact conductance, W/m^2K
H_{mic}	=	microhardness, Pa
$H^{'}$	=	$c_1\,(1.62\sigma'/m)^{c_2}$, Pa
Kn	=	Knudsen number
k	=	thermal conductivity, W/mK
m	=	mean absolute surface slope
M	=	gas parameter, m
n_s	=	number of microcontacts
P	=	pressure, Pa
Pr	=	Prandtl number
Q	=	heat flow rate, W
q	=	heat flux, W/m^2
R	=	thermal resistance, K/W
r, z	=	cylindrical coordinates
T	=	temperature, K
TAC	=	thermal accomodation coefficient
TCR	=	thermal contact resistance
vac.	=	vacuum
Y	=	mean surface plane separation, m

Greek

γ	=	ratio of gas specific heats
Λ	=	mean free path, m
λ	=	non-dimensional separation$\equiv Y/\sqrt{2}\sigma$
σ	=	RMS surface roughness, m
σ'	=	σ/σ_0, $\sigma_0 = 1\ \mu m$

Subscripts

0	=	reference value
1, 2	=	solid 1, 2
a	=	apparent
g	=	gas
j	=	joint
r	=	real
s	=	solid, micro

Introduction

Heat transfer through interfaces formed by mechanical contacts has many important applications such as microelectronics cooling, nuclear engineering, and spacecraft structures design. Generally the heat transfer through the contact interfaces is associated with the presence of interstitial gases. The rate of heat transfer across the joint depends on a number of parameters: thermal properties of solids and gas, gas pressure, surface roughness characteristics, applied load and contact microhardness.

When random rough surfaces are placed in mechanical contact, *real* contact occurs at the top of surface asperities called microcontacts. The microcontacts are distributed randomly in the apparent contact area, A_a, and located far from each other. The real contact area, A_r, the summation of microcontacts forms a small portion of the nominal contact area; typically a few percent of the nominal contact area.

Geometry of a typical conforming rough contact is shown in Fig. 1, where two cylindrical bodies with the radius of b_L are placed in mechanical contact. The gap between the microcontacts is filled with an interstitial

*Ph.D. Candidate, Department of Mechanical Engineering.
†Associate Professor, Director, Microelectronics Heat Transfer Laboratory.
‡Distinguished Professor Emeritus, Department of Mechanical Engineering. Fellow AIAA.

gas and heat is being transferred from one body to another. Conduction through microcontacts and the interstitial gas in the gap between the solids are two main paths for transferring thermal energy between contacting bodies. Thermal radiation across the gap remains small as long as the surface temperatures are not too high, i.e., less than 700 K and in most applications can be neglected.[1] As a result of the small real contact area and low thermal conductivities of interstitial gases, heat flow experiences a relatively large thermal resistance passing through the joint, this phenomenon leads to a relatively high temperature drop across the interface.

Natural convection does not occur within the fluid when the Grashof number is below 2000[2] (the Grashof number can be interpreted as the ratio of buoyancy to viscous forces). In most practical situations concerning thermal contact resistance the gap thickness between two contacting bodies is quite small ($< 0.01mm$), thus the Grashof number based on the gap thickness is less than 2000. Consequently, in most instances the heat transfer through the interstitial gas in the gap occurs by conduction.

In applications where the contact pressure is relatively low, the real contact area is limited to an even smaller portion of the apparent area, in the order of one percent or less. Consequently, the heat transfer takes place mainly through the interstitial gas in the gap. The relative magnitude of the gap heat transfer varies greatly with the applied load, surface roughness, gas pressure and the ratio of the thermal conductivities between the gas and solids. As the contact pressure increases, the heat transfer through the microcontacts increases and becomes more significant. Many engineering applications of thermal contact resistance (TCR) are associated with low contact pressure where air (interstitial gas) is at atmospheric pressure, therefore modeling of the gap resistance is an important issue.

The goal of this study is to develop an approximate comprehensive, yet simple model for determining the heat transfer through the gap between conforming rough surfaces. This model will be used in the second part of this work[3] to develop an analytical compact model for predicting the TCR of non-conforming rough contacts with the presence of an interstitial gas. The model covers the entire range of gas conduction heat transfer modes, i.e., continuum, slip, transition, and free molecular.

Theoretical Background

TCR of conforming rough surfaces with the presence of interstitial gas includes two components, thermal constriction/spreading resistance of microcontacts, R_s, and gap thermal resistance, R_g.

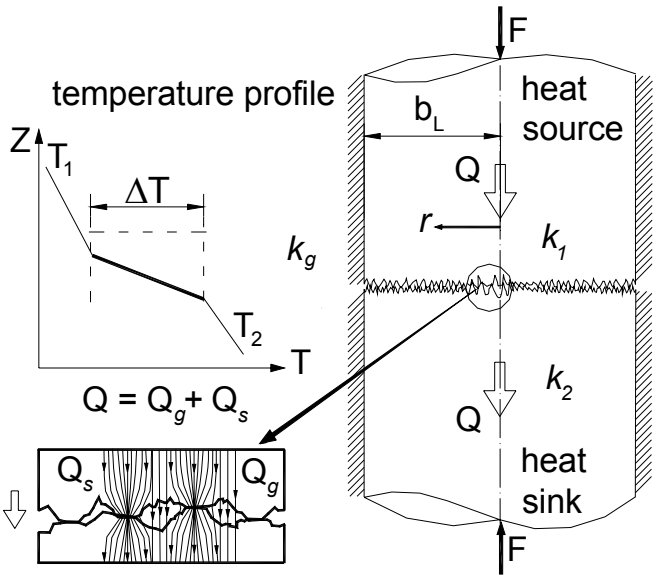

Fig. 1 Contact of conforming rough surfaces with the presence of an interstitial gas

Microcontacts Heat Transfer

All solid surfaces are rough where this roughness or surface texture can be though of as the surface heights deviation from the nominal topography. If the asperities of a surface are isotropic and randomly distributed over the surface, the surface is called Gaussian. Williamson et al.[4] have shown experimentally that many of the techniques used to produce engineering surfaces give a Gaussian distribution of surface heights. Many researchers including Greenwood and Williamson[5] assumed that the contact between two Gaussian rough surfaces can be simplified to the contact between a single Gaussian surface, having an effective surface characteristics, with a perfectly smooth surface, where the mean separation between two contacting planes Y remains the same, see Fig. 2; for more details see Bahrami et al.[6] The equivalent roughness, σ, and surface slope, m, can be found from

$$\sigma = \sqrt{\sigma_1^2 + \sigma_2^2} \quad \text{and} \quad m = \sqrt{m_1^2 + m_2^2} \qquad (1)$$

It is common to assume that the microcontacts are isothermal.[6] Thermal constriction/spreading resistance of microcontacts can be modeled by using the flux tube geometry[7] or if microcontacts are considered to be located far (enough) from each other, the isothermal heat source on a half-space solution[8] can be used. Comparing the above-mentioned solutions, i.e., the flux tube and the half-space, Bahrami et al.[9] showed that the microcontacts can be modeled as heat sources on a half-space for engineering TCR applications.

Bahrami et al.[9] assuming plastically deformed asperities and using scaling analysis techniques devel-

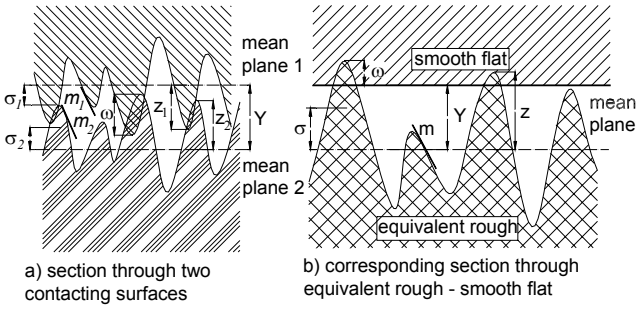

Fig. 2 Equivalent contact of conforming rough surfaces

oped an analytical model to predict TCR of conforming rough contacts in a vacuum, R_s,

$$R_s = \frac{0.565 c_1 \left(\sigma/m\right)}{k_s F} \left(\frac{\sigma'}{m}\right)^{c_2} \tag{2}$$

where,

$$k_s = \frac{2k_1 k_2}{k_1 + k_2}$$

where $\sigma' = \sigma/\sigma_0$ and $\sigma_0 = 1\ \mu m$, c_1, c_2, k_s, and F are a reference value, correlation coefficients determined from the Vickers microhardness measurements, the harmonic mean of solid thermal conductivities, and the applied load, respectively. They compared their model with more than 600 TCR experimental data points collected in a vacuum by many researchers and showed good agreement. The relative RMS difference between Eq. (2) and the data was reported to be approximately 14 percent.

Gap Heat Transfer

According to Springer,[10] conduction heat transfer in a gas layer between two parallel plates is commonly categorized into four heat-flow regimes; continuum, temperature-jump or slip, transition, and free-molecular. The parameter that characterizes the regimes is the Knudsen number

$$Kn = \frac{\Lambda}{d} \tag{3}$$

where Λ and d are the molecular mean free path and the distance separating the two plates, respectively. The molecular mean free path is defined as the average distance a gas molecule travels before it collides with another gas molecule and it is proportional to the gas temperature and inversely proportional to the gas pressure[11]

$$\Lambda = \frac{P_0}{P_g}\frac{T_g}{T_0}\ \Lambda_0 \tag{4}$$

where Λ_0 is the mean free path value at some reference gas temperature and pressure T_0 and P_0.

Figure 3 illustrates the four heat flow regimes, i.e., continuum, temperature-jump or slip, transition, and free-molecular as a function of inverse Knudsen number. In the continuum regime where $Kn \ll 1$, the heat transfer between the plates takes place mainly through the collisions of the gas molecules and the rate of heat transfer is independent of the gas pressure but varies with the gas temperature. Fourier's law of conduction can be used in this regime. As the gas pressure is reduced, the intermolecular collisions become less frequent and the heat exchange of energy between gas molecules and the plates starts to affect the heat transfer between the plates. According to Kenard,[11] for $0.01 \leq Kn \leq 0.1$, the heat exchange exhibits a temperature-jump behavior. The energy transfer between the gas molecules and the plate is incomplete and a discontinuity of temperature develops at the wall-gas interface. At the extreme end of very low gas pressure (or high gas temperature), the free-molecular regime, $Kn \geq 10$, intermolecular collision is rare and the essential mechanism for heat transfer in this regime is the energy exchange between the gas molecules and the plates. The region between the temperature-jump and the free-molecular regime, i.e., $0.1 \leq Kn \leq 10$, is called the transition region in which intermolecular collisions and the energy exchange between the gas molecules and the plate walls are both important.

Using Maxwell's theory for temperature-jump distance, Kenard[11] modelled the gas conduction between two parallel plates for temperature-jump as, $q_g = k_g \left(T_1 - T_2\right) / \left(d + M\right)$. Yovanovich[12] proposed that the Kenard's expression can be used to predict the gas conduction for all four regimes. It can be seen that for the continuum regime $M \to 0$, thus $M \ll d$; also for the free molecular regime $M \to \infty$ and $M \gg d$. Therefore, heat flux for all four flow regimes can be effectively represented by

$$q_g = \frac{k_g}{d + M}\left(T_1 - T_2\right) \tag{5}$$

where T_1, T_2, k_g, and q_g are the uniform temperatures of the two parallel plates, gas thermal conductivity and the gap heat flux, respectively. Using Eq. (5) and the definition of thermal resistance, i.e., $R = \Delta T/Q$, gap thermal resistance can be found from

$$R_g = \frac{d + M}{k_g\ A_g} \tag{6}$$

where $A_g = A_a - A_r$ is the gap heat transfer area. The gas parameter, M, is defined as:

$$M = \left(\frac{2 - TAC_1}{TAC_1} + \frac{2 - TAC_2}{TAC_2}\right)\left(\frac{2\gamma}{1+\gamma}\right)\frac{1}{\mathrm{Pr}}\ \Lambda \tag{7}$$

where TAC_1, TAC_2, γ, Pr, Λ are thermal accommodation coefficients corresponding to the gas-solid

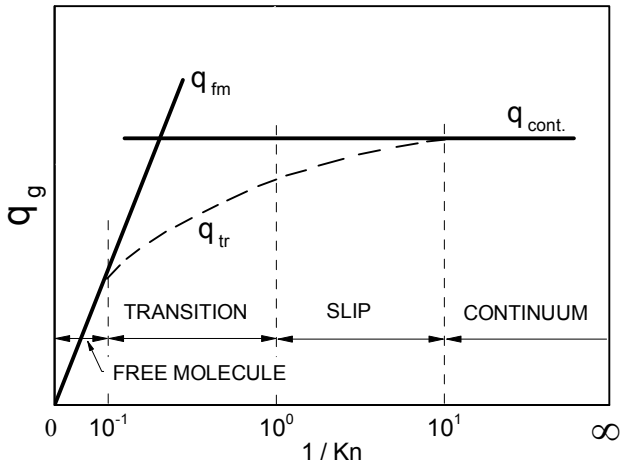

Fig. 3 Heat flux regimes as function of Knudsen number

combination of plates 1 and 2, ratio of the gas specific heats, gas Prandtl number, and molecular mean free path at P_g and T_g, respectively.

Thermal accommodation coefficient, TAC, depends on the type of the gas-solid combination and is in general very sensitive to the condition of the solid surfaces. It represents the degree to which the kinetic energy of a gas molecule is exchanged while in collision with the solid wall. Song and Yovanovich[13] purposed a correlation for predicting TAC for engineering surfaces:

$$TAC = \exp\left[-0.57\left(\frac{T_s - T_0}{T_0}\right)\right]\left(\frac{M_g^*}{6.8 + M_g^*}\right) + \frac{2.4\mu}{(1+\mu)^2}\left\{1 - \exp\left[-0.57\left(\frac{T_s - T_0}{T_0}\right)\right]\right\} \quad (8)$$

where

$$M_g^* = \begin{cases} M_g & \text{for monatomic gases} \\ 1.4M_g & \text{for diatomic/polyatomic gases} \end{cases}$$

where $\mu = M_g/M_s$, M_g, M_s, and $T_0 = 273\ K$ are the ratio of molecular weights, molecular weights of the gas and the solid, and the reference temperature. Equation (8) is general and can be used for any combination of gases and solid surfaces for a wide temperature range. The agreement between the predicted values and the experimental data is within 25 percent.

Yovanovich et al.[14] developed a statistical sophisticated model (we may call it the integral model) to predict thermal gap conductance between conforming rough surfaces. The integral model takes into consideration the variation in the local gap thickness due to the surface roughness. It assumes that the temperature of the two surfaces in contact are uniform and the interface gap consists of many elemental flux tubes of different thermal resistances. The resistances of these elemental flux tubes are then assumed to be in parallel which results in an overall gap conductance in

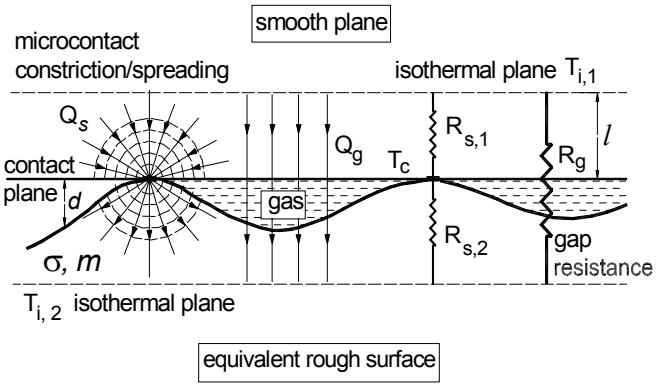

Fig. 4 Microcontacts and gap heat flows, conforming rough contacts

an integral form, that may be represented in thermal resistance form as:

$$R_g = \frac{\sqrt{2\pi}Y}{A_g\ k_g \int_0^\infty \frac{\exp\left[-\left(Y/\sigma - t/\sigma\right)^2/2\right]}{(t/\sigma)/(Y/\sigma) + M/Y} d(t/\sigma)} \quad (9)$$

where R_g, t, k_g, A_g, and Y are thermal gap resistance, length of the elemental flux tube or the local gap thickness, thermal conductivity of the gas, the gap heat transfer area and the mean plane separation distance, respectively.

Equation (9) is in integral form and its evaluation requires a numerical integration. Song[15] correlated Eq. (9) and proposed an expression that can be written as follows:

$$R_g = \frac{Y}{k_g A_g}\left[1 + \frac{0.304\,(\sigma/Y)}{(1 + M/Y)} - \frac{2.29\,(\sigma/Y)^2}{(1 + M/Y)^2} + \frac{M}{Y}\right] \quad (10)$$

Present Model

Implementing the integral model, i.e., Eqs. (9) or (10) in the second part of this study,[3] non-conforming rough contacts with the presence of interstitial gases, resulted in a complicated integral for the effective microgap thermal resistance, which must be solved numerically. Since the main goal of this work is to develop simple compact relationships, an approximate analytical model is developed for predicting the heat transfer of interstitial gases in the gap between conforming rough contacts.

The geometry of the contact is shown in Figs. 1 and 4, the contact of two rough surfaces is simplified to the contact of an equivalent rough and a smooth plate. It is assumed that the contacting surfaces are Gaussian and the asperities deform plastically. Total heat flow through the joint includes the microcontacts Q_s and the gas Q_g.

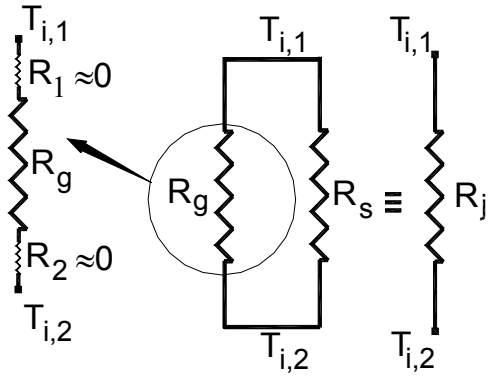

Fig. 5 Thermal resistance network

As previously mentioned, microcontacts can be modeled as isothermal heat sources on a half-space. Considering circular shape microcontacts with the radius a_s in the order of μm, isothermal planes with some temperatures $T_{i,1}$ and $T_{i,2}$ at depth l must exist in bodies one and two, respectively, see Fig. 4. Under vacuum conditions, i.e., $Q_g = 0$ the distance between the isothermal planes and the contact plane is $l = 40a_s \sim 40\ \mu m$.[1] By increasing the gas pressure, heat flow through the joint increases and distance l decreases. Since microcontacts are assumed to be flat and located in the contact plane, isothermal planes $T_{i,1}$ and $T_{i,2}$ are parallel to the contact plane. Therefore TCR can be represented by two sets of thermal resistances in parallel between isothermal planes $T_{i,1}$ and $T_{i,2}$,

$$R_j = \left(\frac{1}{R_s} + \frac{1}{R_g}\right)^{-1} \tag{11}$$

where $R_s = \left(\sum_{i=1}^{n_s} 1/R_{s,i}\right)^{-1}$ and n_s are the equivalent thermal resistance of the microcontacts and the number of microcontacts, respectively. The thermal resistance of the microcontacts R_s is determined using Eq. (2).

Figure 5 shows the thermal resistance network of the joint. Since the thermal resistances are considered to be in parallel between two isothermal plates $T_{i,1}$ and $T_{i,2}$, the gap resistance R_g has three components, the gap resistance and R_1 and R_2, which correspond to the bulk thermal resistance of the solid layers in body 1 and 2, respectively. Considering the fact that the gas thermal conductivity is much lower than solids, i.e., $k_g/k_s \leq 0.01$ and that $l \leq 40\ \mu m$, R_1 and R_2 compared to R_g are negligible, thus one obtains

$$R_{g,\,\text{total}} = \underbrace{\frac{l}{k_{s,1}A_g} + \frac{l}{k_{s,2}A_g}}_{\approx 0} + \frac{d+M}{k_g A_g} = R_g \tag{12}$$

where $A_g = A_a - A_r$ is the gas heat transfer area.

The real contact area is a very small portion of the apparent contact area, i.e., $A_r \ll A_a$, thus it can be assumed $A_g = A_a$. As a result the problem is simplified to the gas heat transfer between two isothermal parallel plates which are located at an effective distance d from each other. In addition, the gap heat transfer area becomes the apparent contact area A_a. As previously mentioned, Eq. (5) can be used to determine the heat transfer between two isothermal parallel plates through an interstitial gas for all four flow regimes.

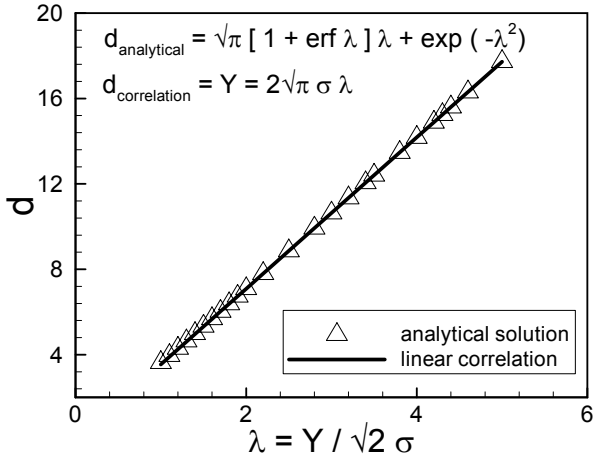

Fig. 6 Comparison between analytical solution and linear correlation of plane separation d

To determine the gap thermal resistance the effective distance between contacting bodies, d, is required. For contact of Gaussian rough surfaces with the mean separation Y, the statistical average plane separation over the contact area, d, can be found from

$$d = \int_{-\infty}^{Y} (Y - z)\ \phi(z)\ dz \tag{13}$$

where $\phi(z)$ is the Gaussian distribution, defined as

$$\phi(z) = \frac{1}{\sqrt{2\pi}\sigma} \exp\left(-\frac{z^2}{2\sigma^2}\right) \tag{14}$$

where z and σ are surface heights and the equivalent RMS surface roughness, respectively. Substituting Eq. (14) into Eq. (13), after evaluating and simplifying, d becomes

$$d = \frac{\sigma}{\sqrt{2\pi}} \left[\sqrt{\pi}\,(1 + \text{erf}\ \lambda)\ \lambda + \exp\left(\lambda^{-2}\right)\right] \tag{15}$$

where $\lambda = Y/\sqrt{2}\sigma$ is the non-dimensional mean separation. Equation (15) is plotted over a wide range of λ, i.e., $1 \leq \lambda \leq 5$ in Fig. 6, a nearly linear behavior can be observed over the comparison range. Thus a linear relationship for d can be derived in the form of

$$d = \sqrt{2}\sigma\lambda = Y \tag{16}$$

The maximum relative difference between Eqs. (15) and (16) is less than 1.7 percent over the entire range

of λ. Equation (16) indicates that d is identical to the mean separation between two planes, i.e., $d = Y$.

For conforming rough contacts assuming plastic deformation of asperities, it can be shown[7]

$$\frac{P}{H_{mic}} = \frac{1}{2}\text{erfc } \lambda \tag{17}$$

or

$$\lambda = \text{erfc}^{-1}\left(\frac{2P}{H_{mic}}\right) \tag{18}$$

where H_{mic}, $P = F/A_a$ and $\text{erfc}^{-1}(\cdot)$ are the effective microhardness of the softer material in contact, contact pressure and inverse complementary error function, respectively.

Microhardness depends on several parameters: mean surface roughness σ, mean absolute slope of asperities, m, type of material, method of surface preparation, and applied pressure. Hegazy[16] proposed correlations in the form of the Vickers microhardness for calculating surface microhardness. Song and Yovanovich[17] developed an explicit expression relating microhardness to the applied pressure

$$\frac{P}{H_{mic}} = \left(\frac{P}{H'}\right)^{\frac{1}{1+0.071c_2}} \tag{19}$$

where $H^{'} = c_1\left(1.62\sigma'/m\right)^{c_2}$, $\sigma' = \sigma/\sigma_0$ and $\sigma_0 = 1$ μm. In situations where an effective value for microhardness $H_{mic,e}$ is known, the microhardness coefficients can be replaced by $c_1 = H_{mic,e}$ and $c_2 = 0$. Substituting Eq. (19) in Eq. (18),

$$\lambda = \frac{Y}{\sqrt{2}\sigma} = \text{erfc}^{-1}\left(\frac{2P}{H'}\right) \tag{20}$$

where for convenience parameter $1/\left(1+0.071c_2\right)$ is assumed to be one, note that $-0.35 \le c_2 \le 0$.

Yovanovich[12] proposed an accurate correlation for determining the inverse complementary error function, $\text{erfc}^{-1}(x) = 0.837\left[-\ln\left(1.566x\right)\right]^{0.547}$ for $x \le 0.01$ with the maximum relative error less than 0.25 percent. Since a broader range of $\text{erfc}^{-1}(\cdot)$ is needed in this study (specially the second part), using Maple[18] a set of expressions for determining $\text{erfc}^{-1}(x)$ are developed which covers a range of $10^{-9} \le x \le 1.9$,

$$\text{erfc}^{-1}(x) = \begin{cases} \dfrac{1}{0.218 + 0.735\ x^{0.173}} & 10^{-9} \le x \le 0.02 \\ \dfrac{1.05\left(0.175\right)^x}{x^{0.12}} & 0.02 < x \le 0.5 \\ \dfrac{1-x}{0.707 + 0.862x - 0.431x^2} & 0.5 < x \le 1.9 \end{cases} \tag{21}$$

The maximum relative difference between Eq. (21) and $\text{erfc}^{-1}(x)$ is less than 2.8 percent for the range of $10^{-9} \le x \le 1.9$. Figure 7 illustrates the comparison between $\text{erfc}^{-1}(x)$ and Eq. (21).

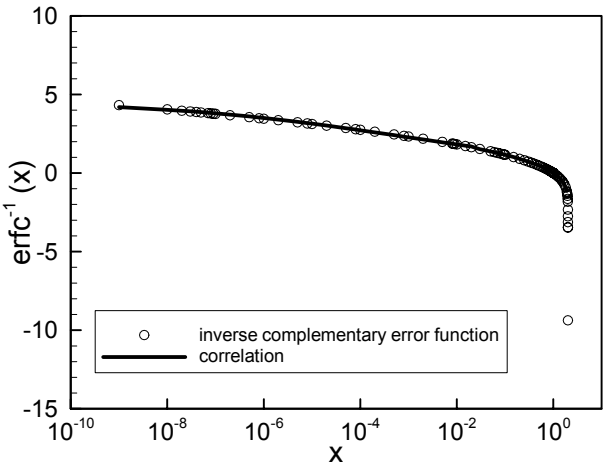

Fig. 7 Inverse complementary error function

Combining Eqs. (16) and (20), the gas thermal resistance can be found from,

$$R_g = \frac{1}{k_g A_a}\left[M + \underbrace{\sqrt{2}\sigma\ \text{erfc}^{-1}\left(\frac{2P}{H'}\right)}_{Y}\right] \tag{22}$$

The thermal joint resistance can be calculated combining Eqs. (11), (2) and (22).

Comparison Between Present and Integral Models

To compare the present model Eq. (22) with the integral model Eq. (10) both expressions are nondimensionalized and re-written in the following form

$$\frac{k_g A_a R_g}{Y} = \begin{cases} 1 + \frac{M}{Y} & \text{Present model} \\ 1 + \dfrac{0.304\left(\frac{\sigma}{Y}\right)}{\left(1+\frac{M}{Y}\right)} - \dfrac{2.29\left(\frac{\sigma}{Y}\right)^2}{\left(1+\frac{M}{Y}\right)^2} + \dfrac{M}{Y} & \text{Song} \end{cases} \tag{23}$$

The ratio, Y/σ, appears in the integral model correlation which can be interpreted as the level of loading; for a fixed contact geometry as the applied load increases Y decreases and this parameter becomes smaller. Three values of Y/σ in Eq. (23) are included in the comparison: 2.5, 3, and 3.5 which represent three levels of loading from high to low, respectively, see Fig. 8. The other parameter, M/Y, is varied over a wide range $\infty > M/Y \le 10^{-3}$ from vacuum to atmospheric pressure condition, respectively. Table 1 lists relative differences between the present and the integral gap models. As can be seen, the relative differences are negligible where $M/Y \ge 1$, i.e., slip to free molecular regimes. As the parameter M/Y becomes smaller, i.e., continuum regime (atmospheric gas pressure condition), the relative difference becomes larger. Observe that the relative difference is larger at smaller values of Y/σ, i.e., higher loads. Remember that the total or joint resistance is the parallel combination

Table 1 Relative percent difference between present and integral gap models

	Y/σ		
M/Y	**3.50**	**3.00**	**2.50**
0.001	9.97	15.26	24.39
0.01	9.63	14.76	23.64
0.10	6.87	10.74	17.48
0.50	1.68	3.04	5.45
1.00	0.17	0.65	1.54
2.00	-0.27	-0.18	0.01
10	-0.06	-0.06	-0.07
20	-0.02	-0.02	-0.02
50	0.00	0.00	0.00
100	0.00	0.00	0.00
6×10^6	0.00	0.00	0.00

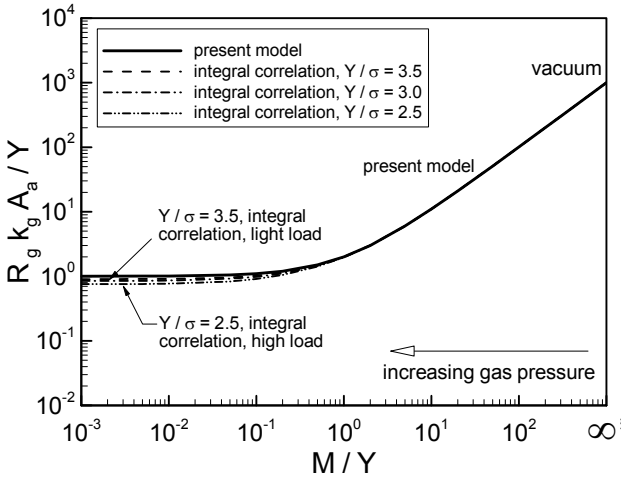

Fig. 8 Comparison of present model with Song correlation

of the microcontact R_s and the gap R_g resistances. It should be noted that the contribution of the gas heat transfer is relatively smaller in higher loads since the microcontact resistance is smaller and controls the joint resistance. As a result, the relative difference in the joint resistances determined from the present and the integral gap models becomes smaller.

Parametric Study

Thermal joint resistance R_j can be non-dimensionalized with respect to the thermal resistance of microcontacts R_s

$$R_j^* = \frac{R_j}{R_s} = \frac{1}{1 + R_s/R_g} \tag{24}$$

Equation (24) is plotted in Fig. 9, in the limit where R_g approaches infinity (vacuum condition), as expected R_j^* approaches one or $R_j = R_s$. As R_s/R_g increases, increasing the gas pressure or at low external loads, R_j^* asymptotically approaches R_g^*.

Effects of external load (applied pressure) and gas pressure on thermal gap and joint resistances are investigated and shown in Figs. 10 and 11, respectively. Input parameters of a typical contact are shown in Table 2, contacting surfaces are stainless steel and the interstitial gas is nitrogen at 373.15 K and 50 $torr$.

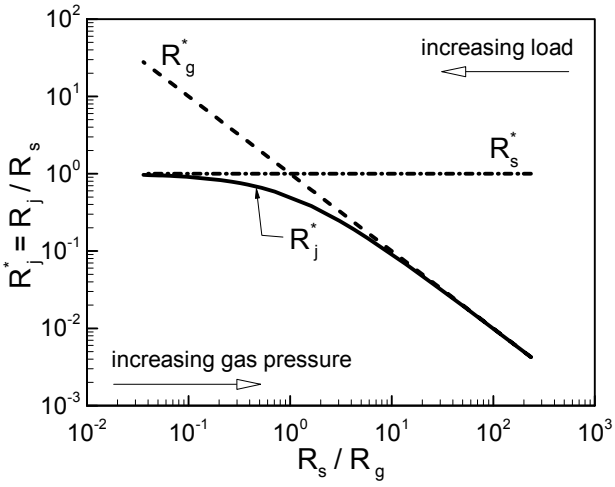

Fig. 9 Non-dimensional thermal joint resistance

Table 2 Input parameters for a typical SS-Nitrogen contact

$TAC_{SS-N_2} = 0.78$	$F = 35\ N$
$b_L = 12.5\ mm$	$\Lambda_0 = 6.28e-9\ m$
$\sigma = 2\ \mu m$	$k_g,\ k_s = 0.031,\ 20\ W/mK$
$m = 0.12$	$c_1,\ c_2 = 6.23\ GPa, -0.23$

The external load is varied over a wide range $10 \leq F \leq 180000\ N$ to study the effect of load on thermal joint resistance. As shown in Fig. 10 at light loads the gap thermal resistance is the controlling component of thermal joint resistance thus most of the heat transfer occurs through the gas. As the load increases, R_s which is inversely proportional to the load, Eq. (2), decreases. As a result, the mean separation between two bodies Y decreases which leads to a decrease in R_g. In higher loads R_s is smaller and controls the joint resistance.

To study the effect of gas pressure on the thermal joint resistance, the gas pressure is varied over the range of $10^{-5} \leq P_g \leq 760\ torr$, while all other parameters in Table 2 are kept constant. As illustrated in Fig. 11, at very low gas pressures (vacuum) R_g is large, thus R_s controls the joint resistance by increasing the gas pressure thermal gas resistance decreases and R_g becomes the controlling component.

Comparison With Experimental Data

The present model is compared with more than 510 experimental data points collected by Hegazy[16] and Song.[15] The geometry of the experimental set up is shown in Fig. 1. Tests include two flat rough cylindrical specimens with the same radius $b_L = 12.5\ mm$ which are placed in contact by applying an external load in a chamber filled with an interstitial gas.

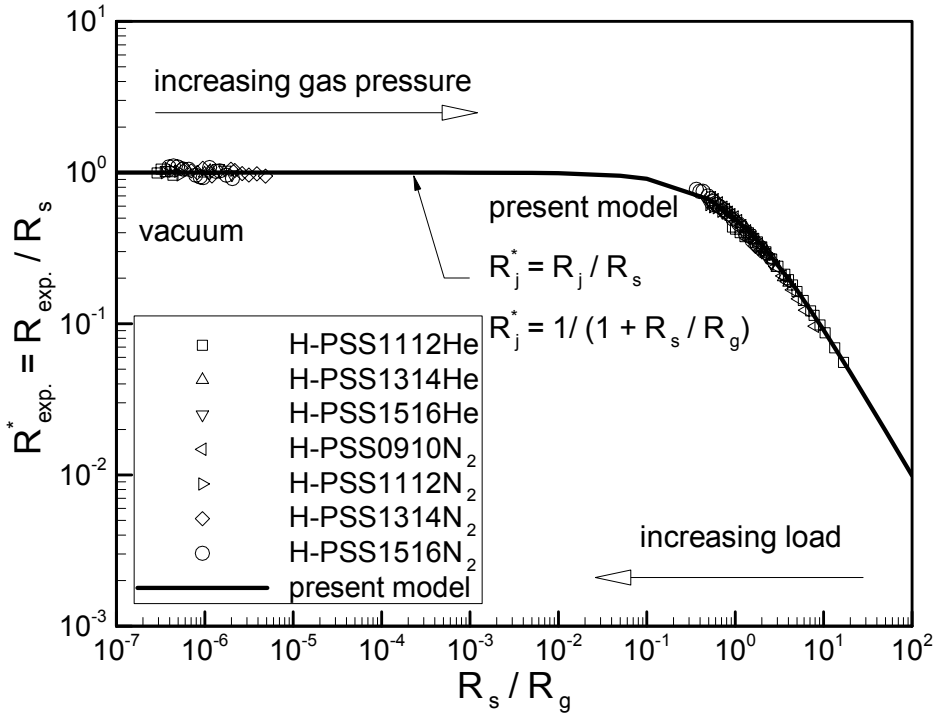

Fig. 12 Comparison of present model with Hegazy data

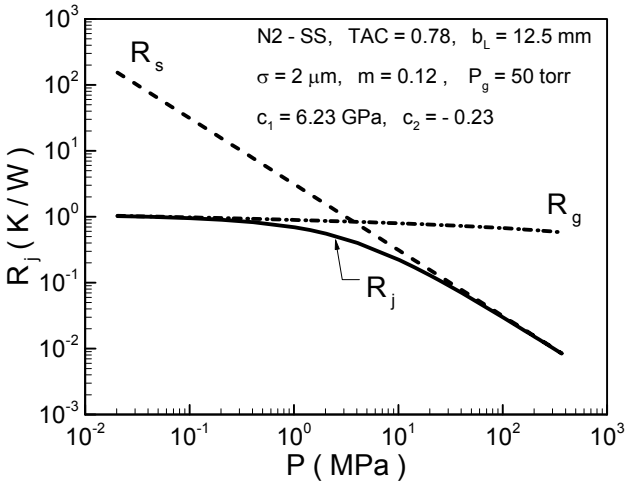

Fig. 10 Effect of load on thermal joint resistance

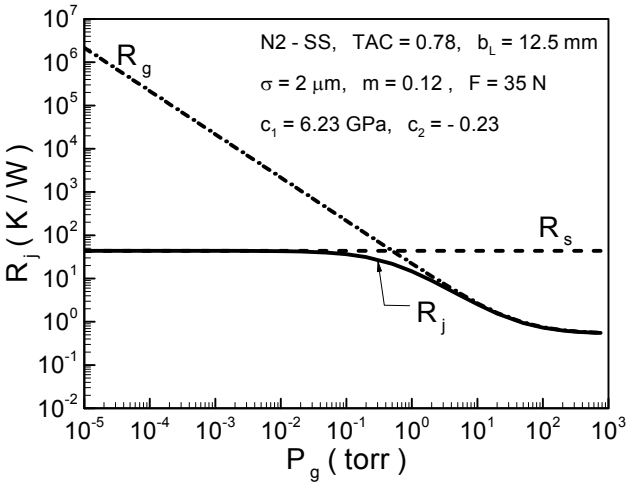

Fig. 11 Effect of gas pressure on thermal joint resistance

To minimize the radiation and convection heat transfer to the surroundings, lateral surfaces of specimens were insulated. Test specimens were made of SS 304 and nickel 200 and interstitial gases were argon, helium, and nitrogen, the gas pressure was varied from atmospheric pressure 760 to vacuum 10^{-5} *torr*. As summarized in Table 3, the experimental data cover a relatively wide range of mechanical, thermal, and surface characteristics.

Thermal properties of argon, helium, and nitrogen are listed in Table 4.[15,16] Note that the reference mean free paths, Λ_0 *nm*, are at 288 *K* and 760 *torr*, and temperature in k_g correlations must be in degree Celsius.

Hegazy[16] Experimental Data

Hegazy[16] collected more than 160 data points during four sets of experiments performed on SS 304 joints tested in nitrogen and helium. Low thermal conductivity, and high microhardness values of SS 304 provides a reasonable set of extremes for verification of the gap model. Table 5 lists the experiment numbers, solid-gas combinations, the gas pressure, surface roughness and slope of the Hegazy experimental data. The nominal contact pressure was varied from 0.459 to 8.769 MPa throughout the tests. The average gas temperature and thermal conductivity of SS 304 were reported in the range of 170 to 220 $^\circ C$ and 20.2 W/mK, respec-

Table 3 Range of parameters for the experimental data

Parameter
$69.7 \leq F \leq 4357\ N$
$0.14 \leq P \leq 8.8\ MPa$
$19.2 \leq k_s \leq 72.5\ W/mK$
$0.08 \leq m \leq 0.205$
$10^{-5} \leq P_g \leq 760\ torr$
$0.55 \leq TAC \leq 0.9$
$1.52 \leq \sigma \leq 11.8\ \mu m$

Table 4 Properties of gases

gas	k_g	Pr	TAC	γ	Λ_0
	W/mK				nm
Ar	0.018+4.05E-5T	0.67	0.90	1.67	66.6
He	0.147+3.24E-4T	0.67	0.55	1.67	186
N_2	0.028+5.84E-5T	0.69	0.78	1.41	62.8

Table 5 Summary of Hegazy experiments

test no.	gas	P_g	σ, m
		$torr$	μm
PSS0910	N_2	562-574	5.65,0.153
PSS1112	N_2, He	vac., 40	5.61,0.151
PSS1314	N_2, He	vac., 40	6.29,0.195
PSS1314	N_2, He	vac., 40	4.02,0.168

tively.

The experimental data are non-dimensionalized and compared with the present model in Fig. 12. The maximum uncertainty of the experimental data was reported to be 5.7 percent. As can be seen in Fig. 12, the present model shows good agreement, the relative RMS difference between the model and the data is approximately 6 percent.

Song[15] Experimental Data

Song[15] conducted seven sets of experiments performed on nickel 200 and SS 304 joints tested in argon, helium and nitrogen. In addition to SS 304 specimens, nickel 200 was chosen which has a thermal conductivity of about 3.5 times that of SS 304 (at 170 $^\circ C$). Thus the contribution of the microcontacts to the joint heat transfer is significantly greater than that of a SS 304 contact of similar conditions. Table 6 summarizes the experiment numbers, solid-gas combinations, range of the nominal contact pressure, and surface roughness and slope of the Song's experimental data. The tests were conducted in the following order: a) at least one vacuum test, b) series of helium tests at various gas pressures, c) vacuum test, d) series of nitrogen tests at various gas pressures, e) vacuum test, and f) series of argon tests at various gas pressures. The gas pressure

Table 6 Summary of Song experiments

test	solid-gas	P	σ, m
		MPa	μm
T1	SS-N_2, SS-Ar, SS-He	0.595-0.615	1.53,0.09
T2	SS-N_2, SS-Ar, SS-He	0.467-0.491	4.83,0.128
T3	Ni-N_2, Ni-Ar, Ni-He	0.511-0.530	2.32,0.126
T4	Ni-N_2, Ni-Ar, Ni-He	0.371-0.389	11.8,0.206
T5	SS-N_2, SS-He	0.403-7.739	6.45/.132
T6	SS-N_2, SS-He	0.526-8.713	2.09,0.904
T7	Ni-N_2, Ni-He	0.367-6.550	11.8,0.206

was varied from 10^{-5} to approximately 650 $torr$. The mean contact temperature, i.e., the mean gas temperature was maintained at approximately 170 $^\circ C$, and the average thermal conductivities of SS 304 and Ni 200 were reported as 19.5 and 71.2 W/mK, respectively.

Experiments T5 through T7 involved gas tests at several load levels, indicated by letters A, B, C, and D in Fig. 13. The purpose of these tests was to observe the load dependence of the thermal gap resistance. As can be seen in Table 6, only helium and nitrogen were used in these tests, since it had been concluded from tests T1 to T4 that argon behaves essentially the same as nitrogen.

Approximately 350 data points are non-dimensionalized and compared with the present model in Fig. 13. The maximum uncertainty of the experimental data was reported to be less than 10 percent. As shown in Fig. 13, present model illustrates good agreement with the data over the entire range of the comparison. The relative RMS difference between the model and the data is 8.1 percent.

Figure 14 illustrates the comparison between the present model and both Hegazy and Song experimental data. The relative RMS difference between the present model and experimental is approximately 7.3 percent.

Concluding Remarks

Heat transfer of an interstitial gas between conforming random rough contacts was studied. Using the general expression for heat transfer between two isothermal parallel plates proposed by Yovanovich,[12] an approximate analytical model was developed. The model covers the four regimes of heat conduction

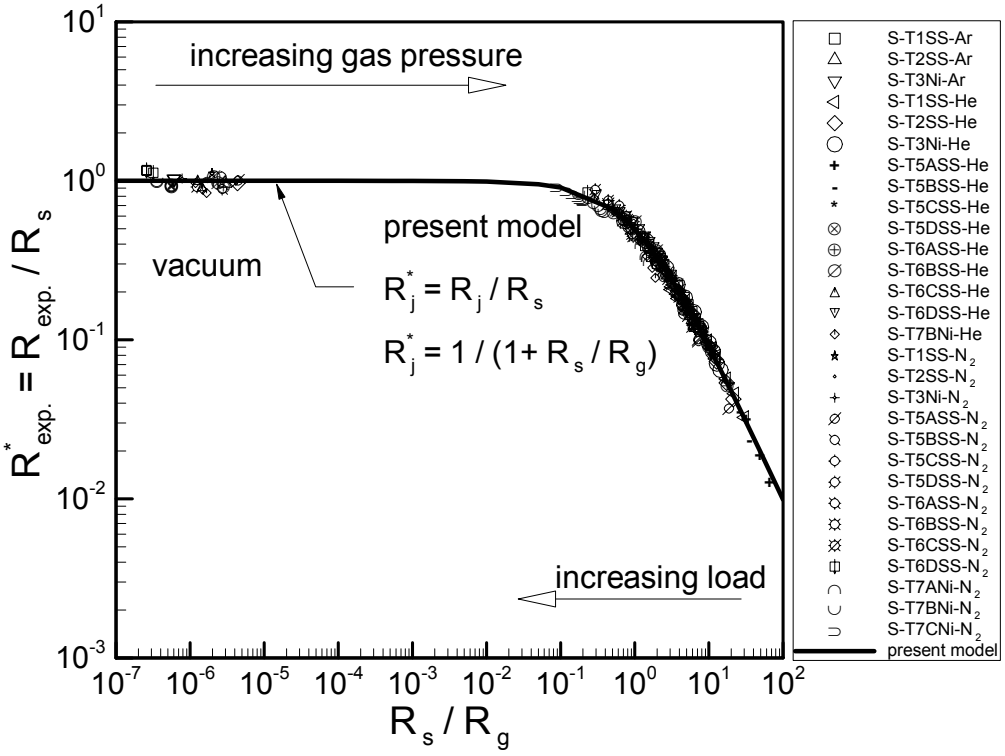

Fig. 13 Comparison of present model with Song data

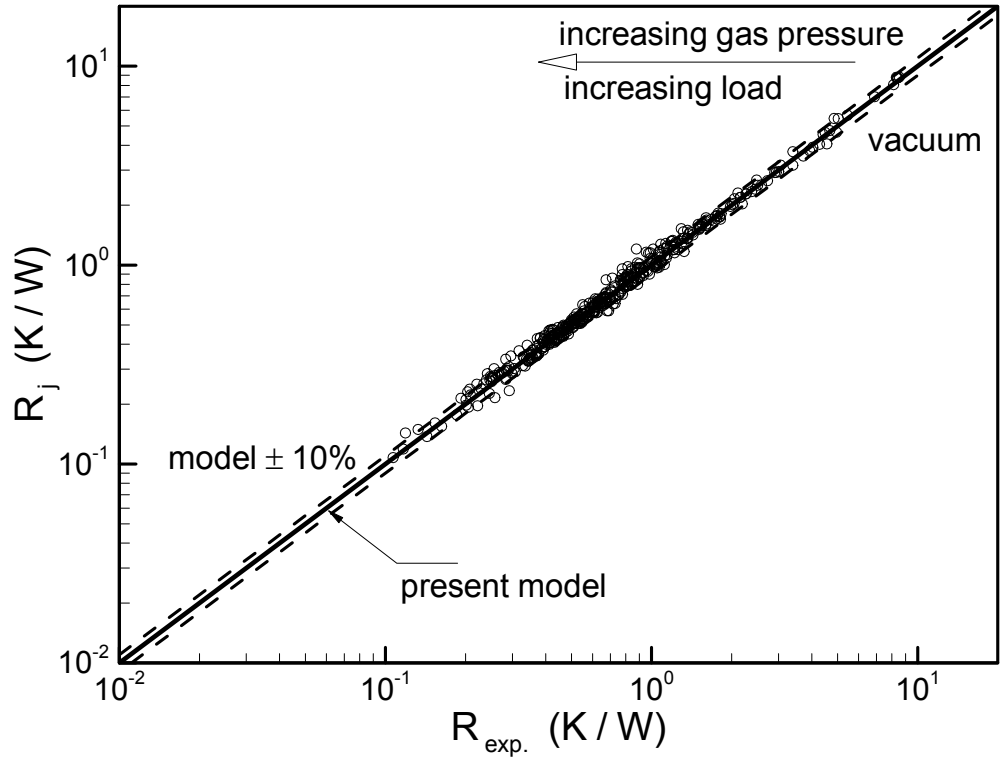

Fig. 14 Comparison present model with Song and Hegazy data

modes of gas, i.e., continuum, temperature-jump or slip, transition, and free molecular and accounts for gas and solid mechanical and thermal properties, gas pressure and temperature, surface roughness, and the applied load.

It was shown that the gas and the microcontacts thermal resistances are in parallel. Using statistical relation for Gaussian rough surfaces, it was illustrated that for engineering applications the average plane separation over the contact area, d, is identical to the mean separation between two contacting surfaces Y. Knowing the real contact area is a very small portion of the apparent area, it was assumed that the gap heat transfer area is identical to the apparent area. Also uniform temperatures for the contacting surfaces were assumed. These assumptions simplified the gap thermal resistance problem and a simple relationship for the gap thermal resistance was derived. A set of simple correlation for inverse complementary error function was developed that determines $\mathrm{erfc}^{-1}(\cdot)$ within 2.8 percent relative error.

Effects of main input parameters on the gap and joint thermal resistances predicted by the model were investigated and shown that

- with constant gas pressure, at light loads R_g was the dominating part of R_j thus most of the heat transfer occurred through the gas. By increasing the external load R_j, R_s and R_g decreased and R_s became relatively smaller and controlled the joint resistance.

- with constant load, at very low gas pressures (vacuum) R_g was large, thus R_s dominated the joint resistance, by increasing the gas pressure R_g decreased and became the controlling component of R_j.

The present model was compared with the integral model, existing model of the Yovanovich et al.,[14] i.e., the Song[15] correlation. It was shown that the relative differences between the present and the integral model were negligible for slip to free molecular regimes. The relative difference became larger for continuum regime (atmospheric gas pressure condition) at relatively high loads. Considering the fact that the contribution of the gas heat transfer is relatively smaller in higher loads, the relative difference in the total joint resistances determined from the present and the integral gap model became smaller.

The present model was compared with more than 510 experimental data points collected by Hegazy[16] and Song.[15] Tests were performed with SS 304 and nickel 200 with three gases, i.e., argon, helium and nitrogen. The data covered a wide range of surface characteristics, applied load, thermal and mechanical properties and the gas pressure, which was varied from vacuum to atmospheric pressure. The present model showed good agreement with the data over entire range of the comparison. The RMS relative difference between the model and data was determined to be approximately 7.3 percent.

References

[1]Bejan, A. and Kraus, D., *Heat Transfer Handbook*, John Willey, New York, 2003.

[2]McAdams, W. H., *Heat Transmission*, McGraw-Hill, New York, 1954.

[3]Bahrami, M., Culham, J. R., and Yovanovich, M. M., "Thermal Resistances of Gaseous Gap for Non-Conforming Rough Contacts," *AIAA Paper No. 2004-0822, 42nd AIAA Aerospace Meeting and Exhibit, Jan 5-8, Reno, Nevada*, 2004.

[4]Williamson, J. B., Pullen, J., Hunt, R. T., and Leonard, D., "The Shape of Solid Surfaces," *Surface Mechanics, ASME, New York*, 1969, pp. 24–35.

[5]Greenwood, J. A. and Williamson, B. P., "Contact of Nominally Flat Surfaces," *Proc., Roy. Soc., London, A295*, 1966, pp. 300–319.

[6]Bahrami, M., Culham, J. R., Yovanovich, M. M., and Schneider, G. E., "Review Of Thermal Joint Resistance Models For Non-Conforming Rough Surfaces In A Vacuum," *Paper No. HT2003-47051, ASME Heat Transfer Conference, July 21-23, Rio Hotel, Las Vegas, Nevada*, 2003.

[7]Cooper, M. G., Mikic, B. B., and Yovanovich, M. M., "Thermal Contact Conductance," *International Journal of Heat and Mass Transfer*, Vol. 12, 1969, pp. 279–300.

[8]Carslaw, H. S. and Jaeger, J. C., *Conduction of Heat in Solids, 2nd. Edition*, Oxford University Press, London, UK, 1959.

[9]Bahrami, M., Culham, J. R., and Yovanovich, M. M., "A Scale Analysis Approach to Thermal Contact Resistance," *Paper No. IMECE2003-44283, 2003 ASME International Mechanical Engineering Congress and RDD Expo, November. 16-21, Washington D.C.*, 2003.

[10]Springer, G. S., "Heat Transfer in Rarefied Gases," *Advances in Heat Transfer, Edited by Irvine T. F. and Hartnett J. P.*, Vol. 7, 1971, pp. 163–218.

[11]Kenard, E. H., *Kinetic Theory of Gases*, McGraw-Hill, New York, London, 1938.

[12]Yovanovich, M. M., "Thermal Contact Correlations," *Progress in Aeronautics and Aerodynamics: Spacecraft Radiative Transfer and Temperature Control, in Horton, T.E. (editor)*, Vol. 83, 1982, pp. 83–95.

[13]Song, S. and Yovanovich, M. M., "Correlation of Thermal Accomodation Coefficient for Engineering Surfaces," *National Heat Transfer Conference, Pittsburgh, PA, August 9-12*, 1987.

[14]Yovanovich, M. M., DeVaal, J. W., and Hegazy, A. A., "A Statistical Model to Predict Thermal Gap Conductance Between Conforming Rough Surfaces," *AIAA Paper No. 82-0888, AIAA/ASME 3rd. Joint Thermophysics, Fluids, Plasma and Heat Transfer Conference, June 7-11, St. Louis, Missouri*, 1982.

[15]Song, S., *Analytical and Experimental Study of Heat Transfer Through Gas Layers of Contact Interfaces*, Ph.D. thesis, University of Waterloo, Dept. of Mech. Eng., Waterloo, Canada, 1988.

[16]Hegazy, A. A., *Thermal Joint Conductance of Conforming Rough Surfaces: Effect of Surface Micro-Hardness Variation*, Ph.D. thesis, University of Waterloo, Dept. of Mech. Eng., Waterloo, Canada, 1985.

[17]Song, S. and Yovanovich, M. M., "Relative Contact Pressure: Dependence on Surface Roughness and Vickers Microhardness," *AIAA Journal of Thermophysics and Heat Transfer*, Vol. 2, No. 1, 1988, pp. 43–47.

[18]Maple7, R., *Waterloo Maple, Release 7*, 2001.